Chemosphere 218 (2019) 147–156

Contents lists available at ScienceDirect

Chemosphere

journal homepage: www.elsevier.com/locate/chemosphere

Uptake of phosphate by *Synechocystis* sp. PCC 6803 in dark conditions: Removal driving force and modeling

Yun Zhou [a, b], Andrew K. Marcus [a], Levi Straka [a], Everett Eustance [a], YenJung Sean Lai [a], Siqing Xia [b, *], Bruce E. Rittmann [a, **]

[a] Biodesign Swette Center for Environmental Biotechnology, Arizona State University, Tempe, AZ 85287-5701, USA
[b] State Key Laboratory of Pollution Control and Resource Reuse, College of Environmental Science and Engineering, Tongji University, Shanghai 200092, China

HIGHLIGHTS

- Uptake of Pi by *Synechocystis* sp. PCC 6803 in dark conditions is investigated.
- Uptake of Pi_{BS} by EPS and IPS were operated in parallel but with different kinetics.
- EPS had a slower Pi-uptake rate but a larger maximum Pi-storage capacity than IPS.
- Protein in EPS and IPS played a key role for binding Pi due to its amine functional groups.
- Biomass with low initial stored Pi had faster Pi-uptake kinetics.

GRAPHICAL ABSTRACT

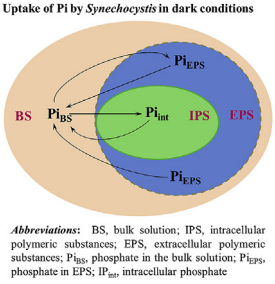

ARTICLE INFO

Article history:
Received 13 March 2018
Received in revised form
11 October 2018
Accepted 8 November 2018
Available online 10 November 2018

Handling Editor: Chang-Ping Yu

Keywords:
Phosphate
Synechocystis

ABSTRACT

Rapid uptake of inorganic phosphate (Pi) by microalgae should occur through two processes operating in parallel: onto extracellular polymeric substances (EPS) and intracellular polymeric substances (IPS). Most previous studies focused only on overall Pi uptake and ignored the roles of EPS. We investigated the two-step removal of Pi by *Synechocystis* sp. PCC 6803 in dark conditions (i.e., without incorporation of Pi into newly synthesized biomass). We also developed a model to simulate both steps. Experimental results with *Synechocystis* confirmed that Pi in the bulk solution was removed by the two uptake mechanisms operating in parallel, but with different kinetics. All uptake rates decreased with time, and the Pi uptake rate by IPS was much higher than that by EPS at all times, but EPS had a larger maximum Pi-storage capacity – 33–48 $mgP/gCOD_{EPS}$ versus 15–17 $mgP/gCOD_{IPS}$. *Synechocystis* had a maximum Pi-storage capacity in the range of 22–28 mgP/g dry biomass. Protein in EPS and IPS played the key role for binding Pi, and biomass with higher protein content had greater Pi-storage capacity. Furthermore,

Abbreviations: EPS, extracellular polymeric substances; SMP, soluble microbial products; IPS, intracellular polymeric substances; Pi, phosphate; EBPR, enhanced biological phosphorus removal; Pi_{BS}, Pi in the bulk solution; Pi_{EPS}, Pi in EPS; Pi_{int}, Pi in IPS; OPi_{int}, intracellular organic phosphate; OPi_{EPS}, organic phosphate in EPS; OPi_{SMP}, organic phosphate in SMP; IPP, intracellular P pool; OD_{730}, optical density at 730 nm; BS, bulk solution; COD, chemical oxygen demand; PCOD, particulate COD; SCOD, soluble COD; BSA, bovine serum albumin.

* Corresponding author.
** Corresponding author.
E-mail addresses: zhouyun06@126.com (Y. Zhou), siqingxia@tongji.edu.cn (S. Xia), Rittmann@asu.edu (B.E. Rittmann).

https://doi.org/10.1016/j.chemosphere.2018.11.056

Uptake model
Extracellular polymeric substances
Intracellular polymeric substances

biomass with low initial stored Pi had faster Pi-uptake kinetics, leading to more Pi removed from the bulk solution. This work lays the foundation for using microalgae as a means to remove Pi from polluted water and for understanding competition for Pi in microbial communities.

1. Introduction

Phosphate (Pi) is an essential nutrient that stimulates the growth of algae and cyanobacteria, particularly in freshwater (Oehmen et al., 2007). Significant sources of Pi entering freshwater include drainage from agricultural land, excreta from livestock, municipal and industrial effluents, and diffuse urban drainage (Lee et al., 1978; Yeoman et al., 1988). Residual Pi leads to algal blooms and eutrophication in aquatic water systems, particularly lakes, reservoirs, and estuaries (Ryther and Dunstan, 1971). Sustainable and cost-effective means for removing Pi from the water bodies would be of high value.

Various technologies have been reported for removing Pi from water. Chemical methods add a divalent (Ca^{2+}) or trivalent (Fe^{3+} and Al^{3+}) metal salt to the water to precipitate metal Pi solids that can be removed by sedimentation or filtration (Yeoman et al., 1988). Enhanced biological phosphorus removal (EBPR) exploits heterotrophic bacteria that can accumulate a high level of internal Pi as polyphosphate when they are cycled through conditions in which they are sequentially starved of electron donor or electron acceptor (Greenberg et al., 1955; Srinath et al., 1959). These Pi-removal processes work well as part of traditional wastewater treatment by activated sludge, but add expense and complexity to wastewater treatment and are not applicable in situations that deviate from traditional wastewater treatment.

Another option for Pi removal is Pi uptake by microalgae. Pi uptake can occur by two distinctly different mechanisms. The first mechanism is incorporation of Pi into the membranes lipids, RNA, DNA, ATP, ADP, NADPH, and $NADP^+$ of newly photosynthesized biomass (Novikoff et al., 1952; Martinez et al., 1999). The second mechanism is adsorption of Pi onto microalgal components. Microalgal biomass includes tertiary amine (≡X-NH+ 3), carboxylic (≡X-COO^-), phosphoryl (≡X-PO- 4), and hydroxyl (≡X-O^-) groups (Zhou et al., 2016c, 2016d, 2017a, 2017b); the positively charged tertiary amines in protein can complex with Pi, as described by these stability reactions:

$$\equiv X - NH_3^+ + H_2PO_4^- \leftrightarrow \equiv X - NH_3H_2PO_4 \quad (1)$$

$$\equiv X - NH_3^+ + HPO_4^{2-} \leftrightarrow \equiv X - NH_4HPO_4^- \quad (2)$$

$$\equiv X - NH_3^+ + PO_4^{3-} \leftrightarrow \equiv X - NH_4HPO_4^{2-} \quad (3)$$

Microalgae, which can take up Pi down to very low concentrations (less than 0.03 mg/L) (Liu and Vyverman, 2015), grow by utilizing solar energy. Thus, Pi removal using microalgae is not restricted to traditional wastewater treatment. The microalgal biomass can be harvested to provide feedstock for biofuels, fish or animal feed, fertilizers, and other valuable products (Aslan and Kapdan, 2006), which opens up the opportunity for Pi removal to be cost effective.

Based on a complete Pi mass balance, Equation (4), previous study (Zhou et al., 2017a) proposed a Pi-uptake and -transformation model during the growth of *Synechocystis* sp. PCC 6803 (hereafter *Synechocystis*):

$$Pi = Pi_{BS} + Pi_{EPS} + Pi_{int} + OPi_{SMP} + OPi_{EPS} + OPi_{int} \quad (4)$$

Initially, Pi in the bulk solution (Pi_{BS}) is rapidly adsorbed by extracellular polymeric substances (EPS) (forming Pi_{EPS}) and intracellular polymeric substances (forming Pi_{int}). As Pi_{BS} is depleted, desorption of Pi_{EPS} become the predominant source for Pi uptake to form Pi_{int}; more Pi_{EPS} is released during EPS hydrolysis. When photosynthesis is active, some of the Pi_{int} is converted into newly synthesized intracellular organic material (forming OPi_{int}). Other parts of Pi_{int} are incorporated into newly generated EPS (OPi_{EPS}), along with soluble microbial products (OPi_{SMP}). In the initial several hours, the key steps are the rapid and simultaneous adsorption of Pi to form Pi_{EPS} and Pi_{int}, and these steps are independent of photosynthesis.

Most previous studies on Pi uptake by microalgae only looked at the global uptake of Pi, not at the distinctly different steps and pools of Pi. In particular, they did not consider the role of EPS for the rapid uptake of Pi and a reservoir of Pi as Pi is depleted in the bulk solution. However, some prior research touched on Pi adsorption. Aslan and Kapdan (2006) mentioned that microalgae's Pi-uptake rate depends on the bulk solution's Pi concentration, the intracellular Pi content, pH, and temperature. Zhang et al. (2013) proposing a metabolic model for the EBPR process, considered the roles of EPS and an intracellular P pool (IPP); however, the metabolic model overlooked important P-associated processes relating to microbial products.

Here, we investigate the uptake of Pi by *Synechocystis* in dark conditions, which accentuates the effects of the initial adsorption steps. We develop a Pi-removal model that is based on two independent and parallel uptake processes, which do not involve photosynthesis: into EPS and intracellular polymeric substances (IPS). Experiments were conducted in dark with *Synechocystis*. The experimental results, which are well represented by the model, confirm two-step removal, the essential role of protein for binding Pi, that microalgae with higher protein content have a greater Pi-storage capacity, and that biomass with initially low initial Pi storage has a faster Pi-uptake rate.

2. Materials and methods

2.1. Cultivation of Synechocystis

Wild-type *Synechocystis* sp. PCC 6803 (hereafter *Synechocystis)* was grown in 1-L Erlenmeyer flasks with a working volume of 700 mL. The medium was standard BG-11 (Rippka et al., 1979). The culturing conditions were: an initial OD_{730} of 0.6 ± 0.02 for the *Synechocystis* inoculum; a temperature of 30 °C maintained by 3 12-W automated-air fans (Minebea-Matsushita Motor Corp., Japan) (Nguyen and Rittmann, 2016); pure CO_2 supplied by sparging with humidified air filtered through the 1.0-μm air filter (Pall, Port Washington, NY, USA); incident light intensity of 276 μmol photons m^{-2} s^{-1}, provided from T5 fluorescent plant grow lamps (Envirogro Hydrofarm, USA); and pH of 8.0 (the same value with our operated photobioreactor) maintained using a pH-Stat that automatically sparged pure CO_2 when the pH was higher than 8.01 (Nguyen and Rittmann, 2015).

A previous study found that the biomass's initial Pi concentration affected the rate and the timing of how Pi was transformed among internal and external sinks (Zhou et al., 2017a). In order to obtain biomass with different Pi characteristics with respect to concentration and distribution of Pi between EPS and IPS, we varied the Pi concentration during biomass cultivation. The baseline condition (called R1) used NO_3–N and PO_4–P concentrations of 120 mg N/L (8.6 mM) and 12 mg Pi/L (0.39 mM), which gave a stoichometric ratio of 22 mol N/mol Pi. We decreased the Pi concentrations to 0.16 mM for condition R2 and to 0.055 mM for condition R3. We prepared the Pi stock solution by dissolving K_2HPO_4 in distilled water to yield a concentration of 5.4 g/L (174 mM). We also augmented the starting alkalinity by adding 6.0 mM of bicarbonate (as $NaHCO_3$). All constituents other than Pi, nitrate, and alkalinity were the same as standard BG-11. Prior to inoculation, the flasks and the BG-11 medium were sterilized by autoclaving, and the pH probe was sterilized using 75% ethanol.

Fig. S1 shows the biomass growth curves during the 9-day incubations. We took samples at 0 h (marked as R1-0h, which is the same sample as R2-0h and R3-0h), 2 h (marked as R1-2h, R2-2h, and R3-2h), 3 days (marked as R1-3d, R2-3d, and R3-3d), and 7 days (marked as R1-7d, R2-7d, and R3-7d). Before we started an adsorption experiment, we centrifuged the culture at 3600×*g* and 4 °C for 10 min and removed the supernatant. We diluted pelleted biomass in deionized (DI) water to give an OD_{730} (optical density at 730 nm) of 0.60.

2.2. Batch experiments of the Pi uptake by Synechocystis

Uptake experiments were carried out by adding the desired volume of the Pi stock solution into 100-mL Erlenmeyer flasks with the working volume of 50 mL. The flask was wrapped with aluminum foil, which ensured that the reaction was carried out in the dark. The initial biomass OD_{730} and Pi concentration were 0.6 and 6 mg/L, respectively. The pH value of the mixed culture was maintained at 8.0 using the pH-8.0 borate buffer, which consists of 0.49 mM H_3BO_3 and 0.2 mM $Na_2B_4O_7 \cdot 10H_2O$ (Wang et al., 2017). The flask was sealed to prevent contamination of the culture during the experiment. The mixture was mixed using one 2-cm magnetic stir bar with a constant rate of 150 rpm and the room temperature was 23.8 °C. Samples were taken with sterile syringes at the noted time and immediately treated and characterized for the Pi concentration in BS, EPS, and I PS (as noted below).

2.3. Separation of Pi in the bulk liquid from external and internal solid components of Synechocystis

Fig. S2 illustrates the centrifugation- and thermal-based methods used to separate Pi in the bulk solution and EPS of *Synechocystis*. We first centrifuged the sample at 10,800×*g* (Microfuge® 22R Centrifuge, Beckman Coulter, CA, USA) and 4 °C for 5 min to separate the particles from the mixed culture. We then collected the supernatant, which provided the bulk solution Pi (Pi_{BS}, mgP/L). We collected the pellets after centrifugation and resuspended them to their original volumes using DI water. The suspensions were heating at 60 °C for 20 min and then centrifuged at 3600×*g* at 4 °C for 15 min. The supernatant was further centrifuged at 10,800×*g* at 4 °C for 10 min to remove all particles, and the collected supernatant contained the EPS (Zhou et al., 2016a, 2017a) and the Pi in EPS (Pi_{EPS}, mgP/L). We then calculated the concentration of intracellular Pi (Pi_{int}, mgP/L) by difference:

$$Pi_{int} = Pi_{Total} - Pi_{BS} - Pi_{EPS} \quad (5)$$

We collected the pellets from the EPS extraction and resuspended them to their original volumes using DI water, and this suspension contained all of the intracellular polymeric substances (IPS). To extract the total intracellular protein and carbohydrate, we mixed 0.2 mL of concentrated nitric acid with 10 mL IPS suspension, and the mixture was shaken at 3200 rpm for 5 h on the Vortex-Genie 2 to completely solubilize the biomass and then centrifuged at 3600×*g* and 23 °C for 10 min to separate the solids. To extract the total intracellular chlorophyll (Gilbert-López et al., 2015), we mixed 1 mL freeze-dried suspension biomass (FreeZone Benchtop instrument (Labconco, MO, USA)) with 3 mL of Folch solvent (Chloroform: methanol = 2:1 v:v) in a 7.5-mL Pyrex disposable screw-cap culture tube. The mixture was subsequently shaken at 3200 rpm for 5 h on the Vortex-Genie 2 and then centrifuged at 3600×*g* and 23 °C for 10 min to separate the solids. We removed 2 mL of supernatant for the total chlorophyll assay. To extract the total intracellular lipid (Sheng et al., 2011; Lai et al., 2016), we mixed 1 mL freeze-dried suspension biomass with 2 mL of 3 N methanolic HCl (Sigma-Aldrich, MO, USA) and incubated at 85 °C in the oven for 2.5 h; we then centrifuged at the mixture at 3600×*g* and 23 °C for 10 min to separate the solids. We removed 1 mL of supernatant for the assay of total lipid.

2.4. Modeling the uptake of Pi by Synechocystis

Surface adsorption is a common kinetic process for the uptake of organic and inorganic solutes by algae (John and Flynn, 2000; Yao et al., 2011). Previous studies (Tien et al., 2005; Rezaee et al., 2006) only focused on overall Pi uptake and used simple equations to describe the uptake process, but ignored the roles of EPS and IPS during Pi adsorption. In this study, we expanded the modeling framework by proposing that Pi binds to cell-bound EPS and intracellular IPS, rather than only on the cell surface. Thus, the uptake of Pi by *Synechocystis* contains five processes that are illustrated in Fig. 1.

2.4.1. Pi in EPS

Bulk-liquid Pi can be adsorbed to the protein's tertiary amine (≡X-NH+ 3) functional groups in the EPS bound on the outside of *Synechocystis* cells (Process I). This adsorbed Pi also can be desorbed back to the bulk solution (BS) (Process II) (Zhou et al., 2017a).

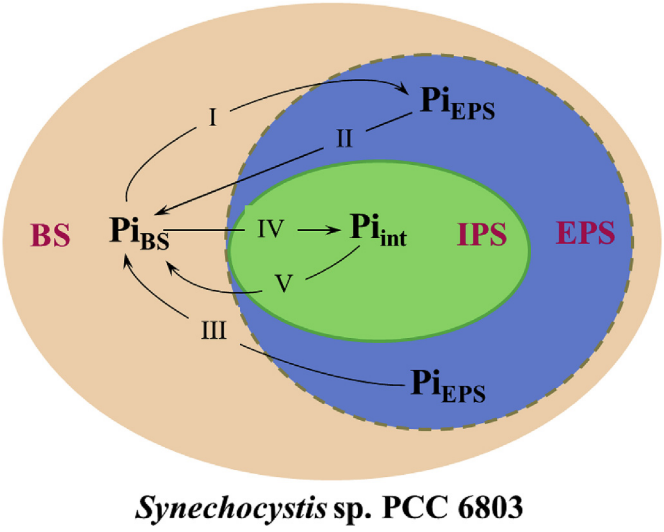

Fig. 1. Proposed model of Pi-uptake processes in dark conditions. Process I, adsorption of Pi_{BS} by EPS; Process II, desorption of Pi from EPS and to be Pi_{BS}; Process III, Pi_{EPS} release to BS during EPS hydrolysis; Process IV, Pi_{BS} transfer into the cell to be Pi_{int}; and process V, Pi_{int} release to the BS (Pi_{BS}) due to cell decay.

Furthermore, Pi bound to EPS is released to the bulk solution when EPS is hydrolyzed (Laspidou and Rittmann, 2002b) (Process III). The adsorption rate ($R_{Pi\text{-}EPS,\ A}$, mgP/L-d) is defined by an adsorption constant (k_a, L/mgP-d), the Pi concentration in the BS (Pi_{BS}, mgP/L), the available capacity of EPS to adsorb Pi ($S_{EPS\text{-}max,\ app} - S_{EPS}$, mgP/mgCOD$_{EPS}$), and the EPS concentration (EPS, mgCOD$_{EPS}$/L):

$$R_{Pi-EPS,\ A} = \left(\frac{dPi_{EPS}}{dt}\right)_A = k_a Pi_{BS}(SEPS - max,\ app - SEPS)EPS \tag{6}$$

where $S_{EPS\text{-}max,\ app}$ (mgP/mgCOD$_{EPS}$) is the apparent maximum adsorption capacity of EPS for Pi, which means all of the binding sites were occupied by Pi, and $SEPS$ (mgP/mgCOD$_{EPS}$) is the concentration of Pi stored in EPS. The desorption rate of Pi ($R_{Pi\text{-}EPS,\ D}$, mg/L-d) is related to the desorption rate (k_d, d^{-1}) and the total concentration of Pi in EPS ($Pi_{EPS} = S_{EPS}{\cdot}EPS$, mgP/L).

$$R_{Pi-EPS,\ D} = \left(\frac{dPi_{EPS}}{dt}\right)_D = k_d S_{EPS}\ EPS \tag{7}$$

The release rate of Pi from EPS ($R_{Pi\text{-}EPS,\ R}$, mg/L-d) is related to Pi concentration in EPS ($Pi_{EPS} = S_{EPS}{\cdot}EPS$, mgP/L) and the EPS hydrolysis rate (k_{hyd}, d^{-1}).

$$R_{Pi-EPS,\ R} = \left(\frac{dPi_{EPS}}{dt}\right)_{hyd} = k_{hyd} S_{EPS}\ EPS \tag{8}$$

Thus, the net rate of Pi accumulation in EPS is:

$$R_{Pi-EPS} = k_a Pi_{BS}(SEPS,\ max - app - SEPS)EPS - k_d S_{EPS}\ EPS - k_{hyd} S_{EPS}\ EPS \tag{9}$$

2.4.2. Intracellular Pi

In dark conditions, Pi in the BS can transfer into the cell by phosphate transporters that are energized by the proton motive force across the cell membrane (Raghothama, 1999; John and Flynn, 2000; Smith et al., 2003). Inside the cell, Pi is adsorbed to amine groups on IPS (Process IV), but without incorporation into newly synthesized biomass (as photosynthesis does not occur without light). The transport rate of Pi ($R_{Pi\text{-}int,\ T}$, mgP/L-d) is defined by a transport constant (k_T, L/mgP-d), Pi$_{BS}$ (mgP/L), the capacity of biomass that is free to store Pi ($Q_{int\text{-}free} = Q_{int\text{-}max,\ app} - Q_{int}$, mgP/mgCOD$_{IPS}$), and the IPS concentration (IPS, mgCOD$_{IPS}$/L).

$$R_{Pi-int,\ T} = \left(\frac{dPi_{int}}{dt}\right)_T = k_T Pi_{BS} Q_{int-free} = k_T Pi_{BS}(Q_{int-max,\ app} - Q_{int})IPS \tag{10}$$

where $Q_{int\text{-}max,\ app}$ (mgP/mgCOD$_{IPS}$) is the apparent maximum storage capacity of IPS for Pi, and Q_{int} (mgP/mgCOD$_{EPS}$) is the concentration of Pi stored in IPS.

Biomass decay could cause the release of intracellular Pi (Process V) (Laspidou and Rittmann, 2002b). The release rate of Pi$_{int}$ ($R_{Pi\text{-}int,\ r}$, mg/L-d) is related to the biomass decay rate (b, min^{-1}), the Pi concentration stored in IPS (Q_{int}, mgP/mgCOD$_{IPS}$)), and the IPS concentration (IPS, mgCOD$_{IPS}$/L).

$$R_{Pi-int,R} = \left(\frac{dPi_{int}}{dt}\right)_R = bQ_{int}IPS \tag{11}$$

Thus, the overall rate of Pi$_{int}$ increase is described by:

$$R_{Pi-int} = k_T Pi_{BS}(Q_{int-max,app} - Q_{int})IPS - bQ_{int}IPS \tag{12}$$

2.4.3. Parameters estimation

The five parameter values (k_a, k_d, k_{hyd}, k_T, and b) were estimated by minimizing the sum of squares of the deviations between the measured data (PCOD, SCOD, Pi$_{BS}$, Pi$_{EPS}$, and Pi$_{int}$) and the model predictions with the objective function:

$$F(p) = \left(\sum_{i=1}^{n}\left(y_{exp,i} - y(p)_i\right)^2\right)^{1/2} \tag{13}$$

where F(P) is the sum of squares of the deviations between the measured data and model outputs, y$_{exp}$ and y(p) are vectors of n measured values and model predictions at time t_i (i from 1 to n), and p is the vector of the model parameters. The model simulation was performed using the planning solving tool of the Excel software.

2.5. Analytical methods

Sample OD$_{730}$ was measured using a UV–vis BioSpec-mini spectrometer (Shimadzu Corp., Japan). Dry weight (DW) was quantified using the total suspended solids assay, Method 2540D in *Standard Methods* (Association, 1998). We measured Pi, contained in Pi$_{Total}$, Pi$_{BS}$, or Pi$_{EPS}$, using the HACH TNT843 kit. We measured the chemical oxygen demand (COD) of biomass (particulate COD,

Table 1
The characteristics of *Synechocystis* used in the uptake experiment in dark conditions.

Sample	PCOD [a] (mg/L)	DW (mg/L)	EPS (mgCOD/L)	S_{EPS} Q_{int} (mgP/mgCOD$_{EPS}$)	(mgP/mgCOD$_{IPS}$)
R1-0h	173 ± 7	124 ± 2	14.7 ± 1.8	9.46 ± 0.95	0.372 ± 0.050
R1-2h	179 ± 5	128 ± 3	15.2 ± 2.4	39.4 ± 1.40	12.3 ± 0.086
R1-3d	235 ± 7	165 ± 1	15.9 ± 2.2	34.0 ± 1.10	1.53 ± 0.11
R1-7d	252 ± 5	182 ± 4	21.5 ± 1.5	33.3 ± 1.30	0.178 ± 0.013
R2-2h	181 ± 3	131 ± 2	15.5 ± 2.1	36.0 ± 2.20	10.7 ± 0.27
R2-3d	232 ± 5	162 ± 4	15.8 ± 1.9	24.3 ± 1.30	0.600 ± 0.12
R2-7d	237 ± 3	168 ± 1	21.0 ± 1.6	5.62 ± 0.76	0.120 ± 0.014
R3-2h	180 ± 4	130 ± 3	15.6 ± 0.9	29.0 ± 1.70	5.04 ± 0.21
R3-3d	229 ± 2	159 ± 2	16.1 ± 1.4	3.35 ± 0.62	0.234 ± 0.023
R3-7d	232 ± 7	164 ± 3	20.9 ± 2.1	0.335 ± 0.10	0.0380 ± 0.010

R2, and R3 are the biomass growth reactors with initial bulk solution's Pi of 12.0 mgP/L, 4.68 mgP/L and 1.69 mgP/L, respectively; R1-0h is the same sample as R2-0h and R3-0h.
[a] PCOD is the particulate chemical oxygen demand; DW is the dry weight of biomass; EPS are extracellular polymeric substances; S_{EPS}, the starting Pi content in EPS, and $S_{EPS} = Pi_{EPS}/EPS$; Q_{int}, the starting intracellular Pi content, and $Q_{int} = Pi_{int}/IPS = Pi_{int}/(PCOD\text{-}EPS_{COD})$. R1.

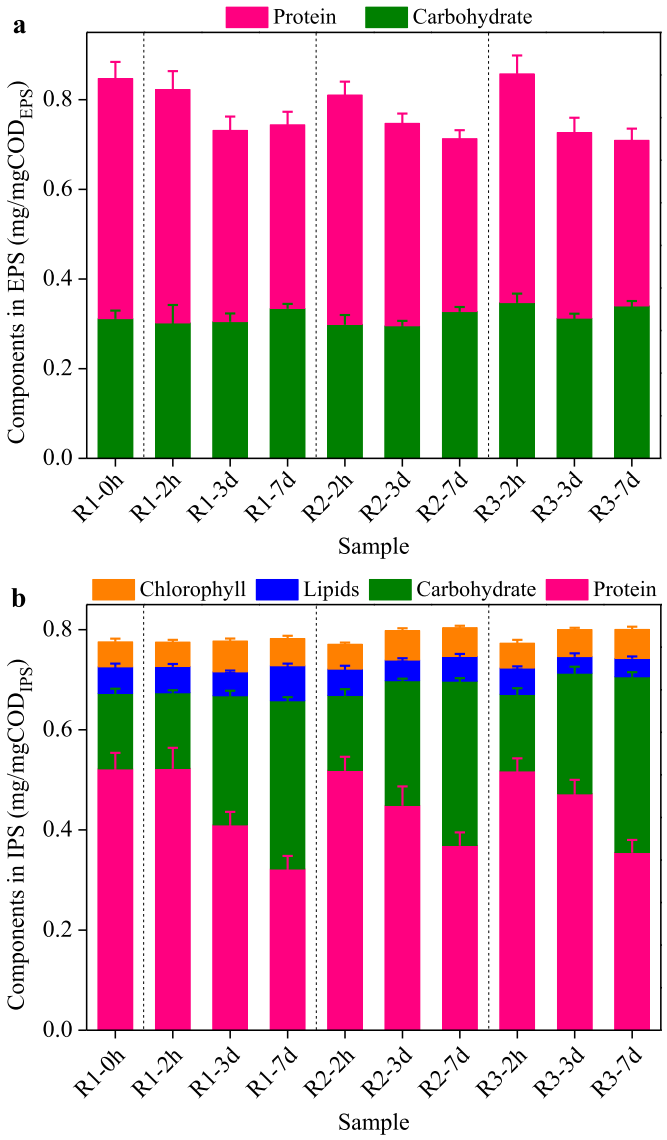

Fig. 2. The components of the EPS and IPS of *Synechocystis* biomass used in the adsorption experiments. R1, R2, and R3 are the biomass growth reactors with initial bulk solution's Pi of 12.0 mgP/L, 4.68 mgP/L, and 1.69 mgP/L, respectively.

PCOD), soluble organic matter in the bulk-solution (soluble COD, SCOD), and in EPS (EPS-COD) using HACH TNT822 kits (0–60 mg/L, Loveland, CO, USA) and a HACH DR2800 spectrophotometer, and the COD for IPS should be PCOD minus EPS-COD. Protein in EPS and IPS was quantified with a QuantiPro BCA Assay Kit (Sigma-Aldrich, St. Louis, MO, U.S.) using bovine serum albumin (BSA) as the standard (Bruce and Perry, 2001). Carbohydrate in EPS and IPS was measured with the phenol-sulfuric acid method using glucose as the standard (Bruce and Perry, 2001). We measured the concentration of chlorophyll with a spectrophotometer (Bio Cary 50 – Varian, USA) based on the characteristic absorbances of chlorophyll at 470 nm (Gilbert-López et al., 2015). The concentration of lipids in IPS was assayed using a gas chromatograph (Shimadzu GC 2010, Japan) equipped with a Supelco SP-2380 capillary column (30 mm × 0.25 mm × 0.20 μm) and flame ionization detector against a 37-Component lipid Mix standard (Supelco, PA, USA). Results are expressed as the mean and standard deviation of three samples (mean ± SD).

3. Results and discussion

3.1. Characteristics of Synechocystis used in this experiment

Table 1 summarizes the biomass and Pi values from all the *Synechocystis* samples. After dilution to the same OD_{730} of 0.6, the biomass concentration (reported as PCOD and DW) and EPS (as COD) were almost the same at the same incubation times for R1, R2, and R3, but the adsorbed Pi contents for EPS and IPS were quite different. EPS and IPS adsorbed more Pi with the highest initial

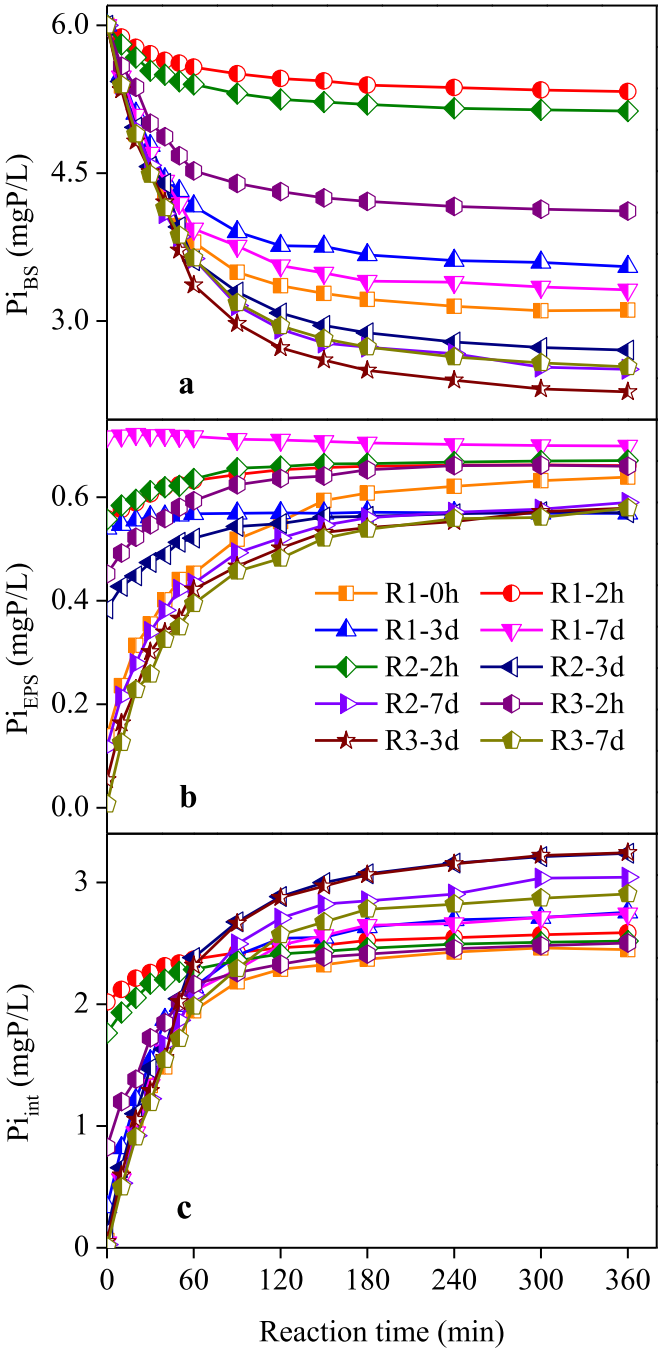

Fig. 3. Changes of Pi in (a) BS, (b) EPS and (c) IPS during batch adsorption experiments with *Synechocystis*. R1, R2, and R3 are the biomass growth reactors with initial bulk solution's Pi of 12.0 mgP/L, 4.68 mgP/L and 1.69 mgP/L, respectively. Characterizations of the biomass for each experiment are in Table 1 and Fig. 2.

bulk-solution Pi after 2 h (R1). While Pi_{EPS} remained after 7 d in R1, it was almost depleted after 3 d in R3.

Fig. 2 shows the components of EPS and IPS. All of the components in EPS and IPS had almost the same concentration at the same incubation times for R1, R2, and R3. Protein in EPS declined over time, but carbohydrates remained almost constant. In the IPS of *Synechocystis*, protein declined over time, but carbohydrate gradually increased. The concentrations of lipids and chlorophyll were about 0.05 mg/mgCOD_{IPS} and remained stable over time.

3.2. Adsorption of Pi by Synechocystis in dark conditions

Fig. 3 shows the time course for the adsorption of Pi by *Synechocystis* in dark conditions. Pi_{BS}, Pi_{EPS}, and Pi_{int} had two similar trends in most of the experiments. (1) Within the first 180 min, Pi_{EPS} and Pi_{int} steadily increased in parallel to decreasing Pi_{BS}. While this trend was consistent, the rates varied widely. (2) A steady-state was established after ~240 min. At steady-state, Pi_{int} was much higher than Pi_{EPS}, meaning most Pi ultimately was adsorbed inside the cells. However, the adsorbed amounts varied among the experiments.

Fig. 4 presents relationships showing how the initial Pi concentration affected Pi uptake amount and rate in EPS, IPS, and the whole biomass. A high initial value for adsorbed Pi slowed the Pi-uptake rate in EPS, IPS, and the whole biomass. All Pi-uptake rates decreased with time, and the Pi uptake rate by IPS was much higher than that by EPS at any time. The initial adsorbed Pi had a strong and nearly linear negative relationship with the captured amount of Pi in EPS ($R^2 = 0.96$, $P < 0.01$), IPS ($R^2 = 0.92$, $P < 0.01$), and the whole biomass ($R^2 = 0.95$, $P < 0.01$). Overall, high initial stored Pi in EPS, IPS, and *Synechocystis* led to less removal of Pi from the bulk solution.

3.3. Experiment results fit to the two-step Pi-uptake model

The two-step Pi-uptake model was calibrated and compared with experimental data. Fig. 5 (a)-(c) compares the experimental data and simulation results for Pi_{BS}, Pi_{EPS} and Pi_{int}, and Table 2

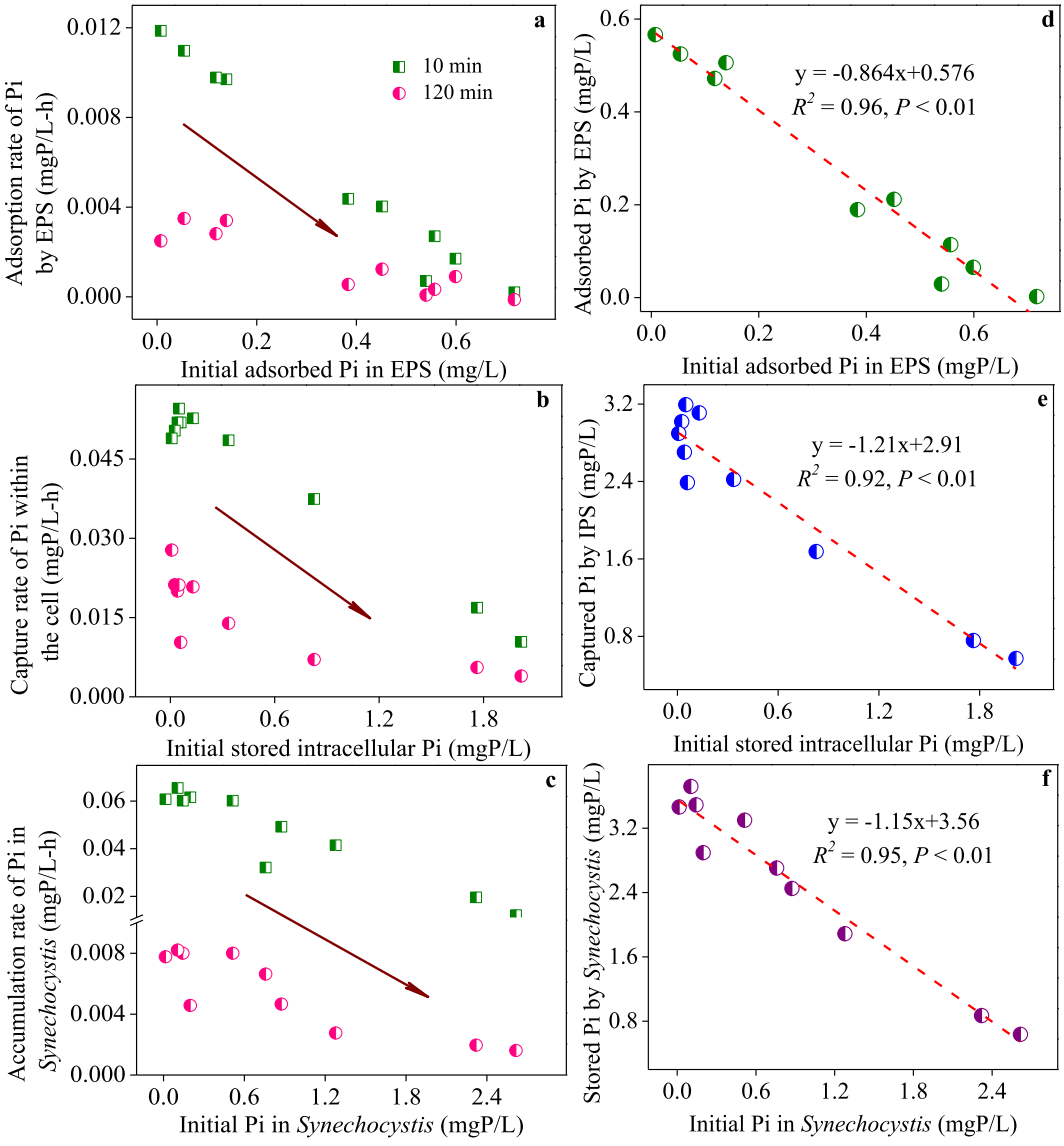

Fig. 4. Relationships between the initial adsorbed Pi concentration and the Pi uptake rate at 10 min and 120 min (left) and Pi uptake amount after 300 min (right) in EPS, IPS and the whole biomass. Primary data are in Fig. 2.

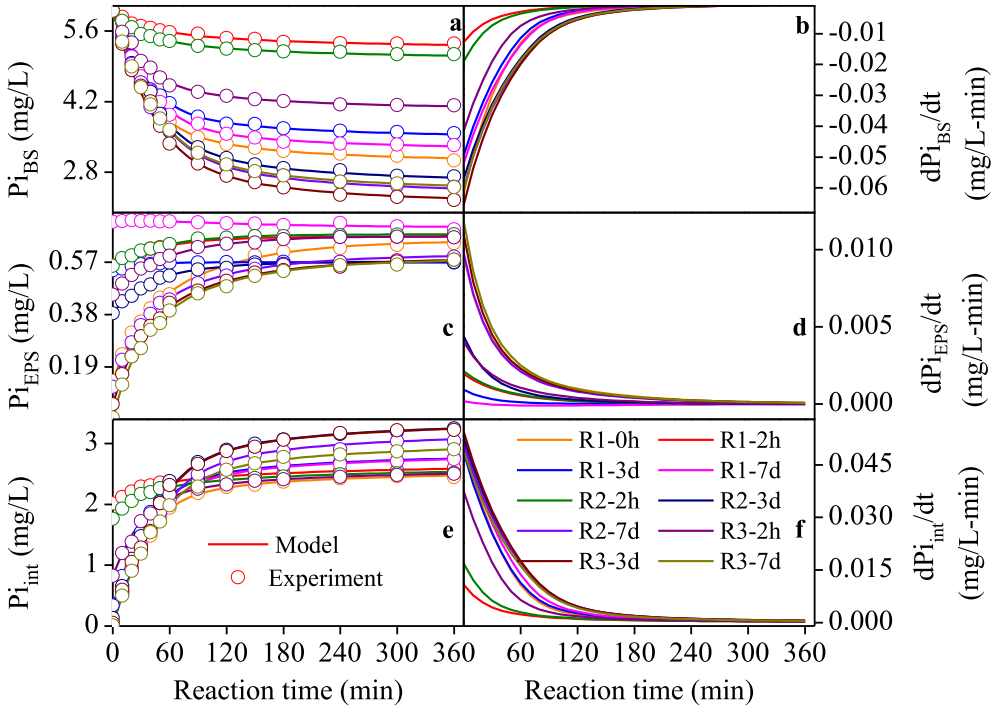

Fig. 5. Comparison of the model outputs and experimental data for the concentration and variation rate of Pi in the bulk solution, EPS and within the cells of *Synechocystis*.

summarizes the parameter values. The model results in Fig. 5 (a)-(c) match all experimental results closely and without systematic error for any parameter. Quantitative matching of experimental and modeled results for all three forms of Pi is strong evidence that the two-step Pi-adsorption model represents the experimental results accurately. The values for parameters k_{hyd} and b for *Synechocystis* were 0.161 d^{-1} and 0.0631 d^{-1}, respectively, which are almost the same as for previous studies (Wanner and Gujer, 1986; Laspidou and Rittmann, 2002a), another piece of evidence that the model is well formulated.

Fig. 5 (d)-(f) show the modeled Pi transfer rates from or to BS, EPS, and IPS. The Pi transfer rates gradually decreased over time, and higher initial Pi slowed the Pi-adsorption rate, which agrees with the experimental data in Fig. 3. The Pi-adsorption rate by IPS was much higher than that of by EPS at all times, and the rates of adsorption by EPS and IPS followed different patterns over the course of the experiments. These trends confirm that the Pi uptake by EPS and IPS were independent processes, as represented in the two-step model.

Table 3 summarizes the experimental and modeled amounts of adsorbed Pi after 360 min. Model outputs for the maximum stored Pi are slightly higher than the experimental data for EPS and IPS. The explanation is that the experimental data of Pi in EPS and IPS did not reach the true maxima at 360 min, a result consistent with previous reports (Zhou et al., 2016b, 2016c). The experimental data and model outputs for $S_{EPS\text{-}max,app}$ gradually decreased over time no matter whether the initial Pi was high or low. Additionally, the model outputs show that EPS and IPS had maximum Pi storage capacities in the ranges of 33–48 mgP/$gCOD_{EPS}$ and 15–17 mgP/$gCOD_{IPS}$, respectively. *Synechocystis* had a maximum Pi-storage capacity in the range of 22–28 mgP/g dry biomass. Thus, EPS had greater Pi-storage capacity.

Table 2
Parameter values for the two-step Pi-adsorption model [a].

Parameters	k_a	k_d	k_{hyd}	k_T	b
Units	L/mg-d	d^{-1}	d^{-1}	L/mg-d	d^{-1}
Value	3.57	2.33	0.161	6.02	0.0631

[a] k_a (L/mg-d) and k_d (d^{-1}) are the adsorption and desorption constants, respectively; k_{hyd} (d^{-1}) is the EPS hydrolysis rate; k_T (L/mg-d) is the transfer constant; b (d^{-1}) is the biomass decay rate.

3.4. Uptake capacity of Synechocystis EPS and IPS for Pi

Fig. 6 (a) and (b) show the Pearson correlations between the apparent maximum amount of stored Pi (model outputs with the maximum parameter values and experimental data after adsorbed for 360 min) and the concentrations of protein and carbohydrate in EPS. Pi in EPS had a strong and nearly linear relationship ($R^2 > 0.98$, $P < 0.01$) with the protein content in EPS. In contrast, the linear regression between the concentrations of Pi and carbohydrate in EPS was not significant ($R^2 < 0.61$, $P > 0.08$). Thus, the EPS results

Table 3
The stored Pi in EPS and IPS for model outputs with the maximum parameter values and experimental data after adsorbed for 360 min [a].

Sample number	$S_{EPS\text{-}max,app}$ (mgP/$gCOD_{EPS}$)		$Q_{int\text{-}max,app}$ (mgP/$gCOD_{IPS}$)	
	Experiment	Model	Experiment	Model
R1-0h	44	48	14	17
R1-2h	44	45	15	17
R1-3d	36	38	12	16
R1-7d	31	34	11	15
R2-2h	43	44	14	17
R2-3d	36	40	14	17
R2-7d	28	33	13	16
R3-2h	43	44	14	17
R3-3d	32	36	14	17
R3-7d	29	33	13	16

[a] $S_{pmax\text{-}app}$ (mgP/$gCOD_{EPS}$) is the apparent maximum amount of adsorbed Pi by EPS, $S_{EPS\text{-}max,\ app} = Pi_{EPS\text{-}max}$/EPS; $Q_{int\text{-}max,\ app}$ (mgP/$gCOD_{IPS}$) is the apparent maximum stored Pi in IPS, $Q_{int\text{-}max,\ app} = Pi_{int\text{-}max}$/PCOD.

support that the amine groups in the protein of EPS played the key role in the binding of Pi (Deo et al., 2010; Zhou et al., 2017a).

Fig. 6 (c)-(f) represent the Pearson correlations between the apparent maximum stored Pi in IPS (model outputs with the maximum parameter values and experimental data after adsorbed for 360 min) and the concentrations of intracellular protein, carbohydrate, lipids, and chlorophyll. Similar to EPS, the apparent maximum stored Pi in IPS correlated with protein ($R^2 > 0.792$, $P < 0.01$), but not with carbohydrate ($R^2 < 0.53$, $P \geq 0.09$), lipids ($R^2 < 0.22$, $P \geq 0.18$), or chlorophyll ($R^2 < 0.37$, $P \geq 0.12$). Again, amine groups in the protein of IPS controlled the Pi adsorption and storage inside *Synechocystis*.

3.5. Implications of this work

Our results confirm that protein in EPS and IPS played the key

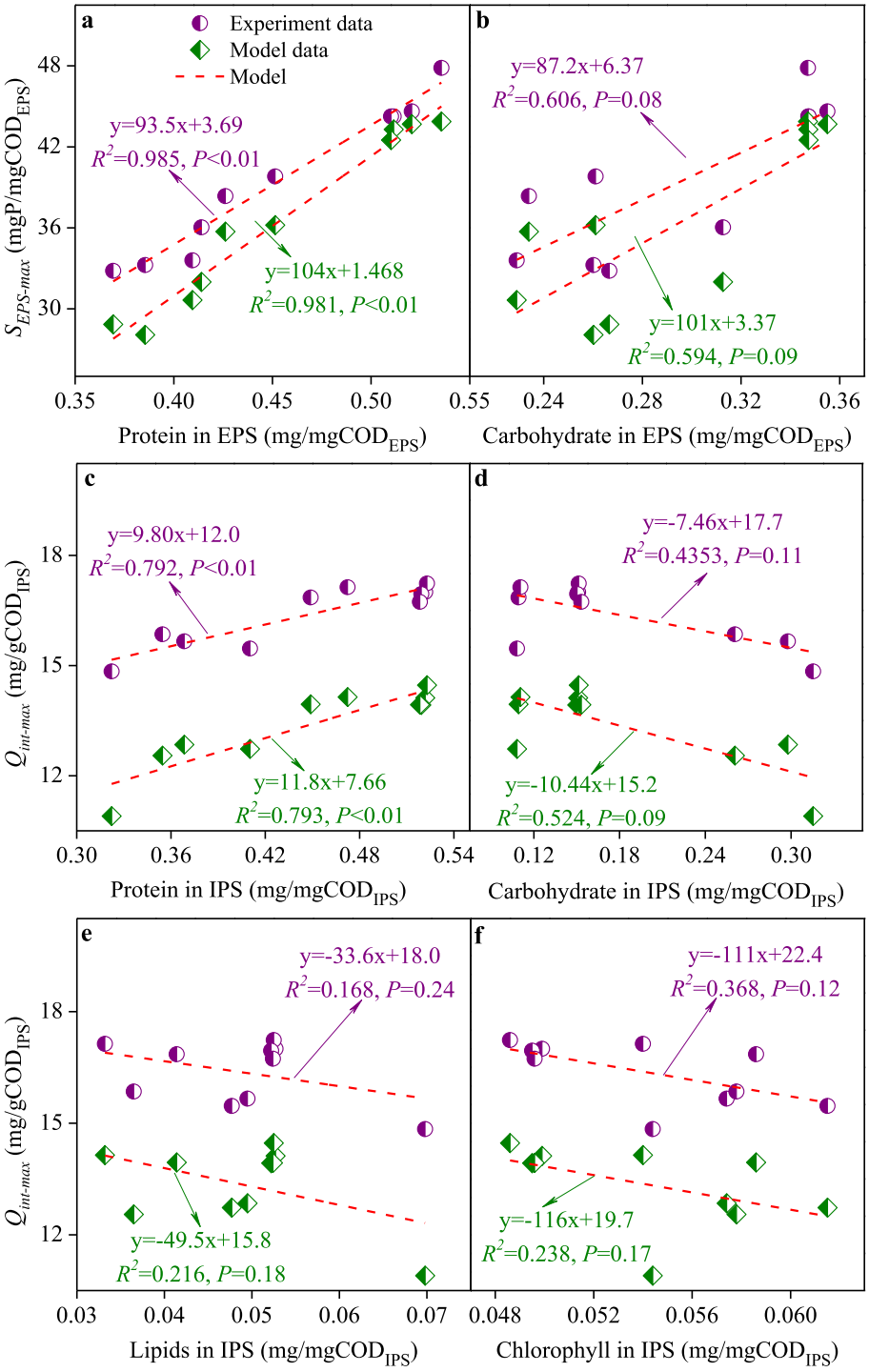

Fig. 6. Pearson correlations between the apparent maximum amounts of adsorbed Pi by EPS and the proportions of (a) protein and (b) carbohydrate in EPS, and the apparent maximum stored Pi in IPS (model outputs with the maximum parameter values and experimental data after adsorbed for 360 min) and the concentrations of intracellular (c) protein, (d) carbohydrate, (e) lipids and (f) chlorophyll.

role for adsorbing Pi due to its amine functional groups. Therefore, microalgae with higher protein content have a greater Pi-storage capacity. Low initial stored Pi in the biomass led to a faster Pi-uptake rate and greater removal of Pi from the bulk solution. Thus, microalgae with high protein content and low initial stored Pi could be useful as a rapid and high-capacity adsorbent for the removal of Pi.

A number of factors can affect the protein content in microalgae, including light intensity, nitrogen concentration, temperature, and the growth phase. A common trend is that microalgae increase their content of protein, primary carotenoids and chlorophylls (contain chlorophyll *a, b and c*) in response to decreasing light intensity (Hu, 2004). In conditions of high light intensity and nitrogen limitation, protein is replaced by lipids and/or carbohydrates (Dean et al., 2010). Furthermore, a decrease in growth temperature below the microalgae's optimal range also may result in increasing protein production, especially for enzymes associated with adaptions to maintain rates of photosynthesis and respiration (Thompson et al., 1992). Thus, low light intensity and low temperature may lead to a high protein content of microalgae.

The two-step model for Pi-uptake, which represented the experimental data well for dark conditions, lays the foundation to build a more comprehensive model that also includes the dynamics of how microalgae transform Pi into organic P when exposed to light. Such a model can be applied to understanding microbial communities in natural systems and for using microalgae as a means to remove Pi from polluted water.

4. Conclusions

Investigating the uptake of Pi by *Synechocystis* in dark conditions, we found that Pi in BS was removed by two rapid uptake mechanisms – onto EPS and IPS – that operated in parallel, but with different kinetics. A two-step model for Pi uptake represented the experimental data well. A high initial value for stored Pi slowed the Pi-uptake rates, leading to a lower amount of Pi removal from the BS. All uptake rates decreased with time, and the Pi uptake rate by IPS was much higher than that of by EPS at all times. However, EPS had greater Pi uptake capacity – 33–48 mgP/gCOD$_{EPS}$ – than IPS – 15–17 mgP/gCOD$_{IPS}$. Protein in EPS and IPS played the key role in binding Pi; biomass with higher protein content had greater Pi storage capacity and uptake rate. This work lays the foundation for using microalgae as a means to remove Pi from polluted water and for understanding competition for Pi in microbial communities.

Acknowledgements

This work was supported by LightWorks, Arizona State University, and part by China Scholarship Council (201506260022), National Science Foundation of China (51678422, 51378368), National Key Research and Development program of China (2017YFC0403403), and Shanghai Tongji Gao Tingyao Environmental Science & Technology Development Foundation. We thank Dr. Willem Vermaas and his laboratory in the School of Life Sciences at Arizona State University for providing *Synechocystis* sp. PCC6803 wild type.

Appendix A. Supplementary data

Supplementary data to this article can be found online at https://doi.org/10.1016/j.chemosphere.2018.11.056.

References

Aslan, S., Kapdan, I.K., 2006. Batch kinetics of nitrogen and phosphorus removal from synthetic wastewater by algae. Ecol. Eng. 28, 64–70.
Association, A.P.H., 1998. Standard Methods for the Examination of Water and Wastewater. American Public Health Association, Washington, DC, p. 1268.
Bruce, E.R., Perry, L.M., 2001. Environmental Biotechnology: Principles and Applications. McGrawHill, New York, p. 400.
Dean, A.P., Sigee, D.C., Estrada, B., Pittman, J.K., 2010. Using FTIR spectroscopy for rapid determination of lipid accumulation in response to nitrogen limitation in freshwater microalgae. Bioresour. Technol. 101, 4499–4507.
Deo, R.P., Songkasiri, W., Rittmann, B.E., Reed, D.T., 2010. Surface complexation of neptunium (V) onto whole cells and cell components of Shewanella alga: modeling and experimental study. Environ. Sci. Technol. 44, 4930–4935.
Gilbert-López, B., Mendiola, J.A., Fontecha, J., van den Broek, L.A.M., Sijtsma, L., Cifuentes, A., Herrero, M., Ibáñez, E., 2015. Downstream processing of Isochrysis galbana: a step towards microalgal biorefinery. Green Chem. 17, 4599–4609.
Greenberg, A.E., Klein, G., Kaufman, W.J., 1955. Effect of phosphorus on the activated sludge process. Sewage Ind. Wastes 277–282.
Hu, Q., 2004. Environmental Effects on Cell Composition. Blackwell Science Ltd., Oxford, UK.
John, E.H., Flynn, K.J., 2000. Modelling phosphate transport and assimilation in microalgae; how much complexity is warranted? Ecol. Model. 125, 145–157.
Lai, Y.S., Zhou, Y., Martarella, R., Wang, Z., Rittmann, B.E., 2016. Synergistic integration of C12–C16 cationic surfactants for flocculation and lipid extraction from chlorella biomass. ACS Sustain. Chem. Eng. 5, 752–757.
Laspidou, C.S., Rittmann, B.E., 2002a. Non-steady state modeling of extracellular polymeric substances, soluble microbial products, and active and inert biomass. Water Res. 36, 1983–1992.
Laspidou, C.S., Rittmann, B.E., 2002b. A unified theory for extracellular polymeric substances, soluble microbial products, and active and inert biomass. Water Res. 36, 2711–2720.
Lee, G.F., Rast, W., Jones, R.A., 1978. Water Report: eutrophication of water bodies: insights for an age old problem. Environ. Sci. Technol. 12, 900–908.
Liu, J., Vyverman, W., 2015. Differences in nutrient uptake capacity of the benthic filamentous algae Cladophora sp., Klebsormidium sp. and Pseudanabaena sp. under varying N/P conditions. Bioresour. Technol. 179, 234–242.
Martinez, M.E., Jimenez, J.M., El Yousfi, F., 1999. Influence of phosphorus concentration and temperature on growth and phosphorus uptake by the microalga Scenedesmus obliquus. Bioresour. Technol. 67, 233–240.
Nguyen, B.T., Rittmann, B.E., 2015. Predicting dissolved inorganic carbon in photoautotrophic microalgae culture via the nitrogen source. Environ. Sci. Technol. 49, 9826–9831.
Nguyen, B.T., Rittmann, B.E., 2016. Effects of inorganic carbon and pH on growth kinetics of Synechocystis sp. PCC 6803. Algal Res. 19, 363–369.
Novikoff, A.B., Hecht, L., Podber, E., Ryan, J., 1952. Phosphatases of rat liver I. The dephosphorylation of adenosinetriphosphate. J. Biol. Chem. 194, 153–170.
Oehmen, A., Lemos, P.C., Carvalho, G., Yuan, Z., Keller, J., Blackall, L.L., Reis, M.A.M., 2007. Advances in enhanced biological phosphorus removal: from micro to macro scale. Water Res. 41, 2271–2300.
Raghothama, K.G., 1999. Phosphate acquisition. Annu. Rev. Plant Biol. 50, 665–693.
Rezaee, A., Ramavandi, B., Ganati, F., 2006. Equilibrium and spectroscopic studies on biosorption of mercury by algae biomass. Pakistan J. Biol. Sci. 9, 777–782.
Rippka, R., Deruelles, J., Waterbury, J.B., Herdman, M., Stanier, R.Y., 1979. Generic assignments, strain histories and properties of pure cultures of cyanobacteria. Microbiology 111, 1–61.
Ryther, J.H., Dunstan, W.M., 1971. Nitrogen, phosphorus, and eutrophication in the coastal marine environment. Science 171, 1008–1013.
Sheng, J., Vannela, R., Rittmann, B.E., 2011. Evaluation of cell-disruption effects of pulsed-electric-field treatment of *Synechocystis* PCC 6803. Environ. Sci. Technol. 45, 3795–3802.
Smith, S.E., Smith, F.A., Jakobsen, I., 2003. Mycorrhizal fungi can dominate phosphate supply to plants irrespective of growth responses. Plant Physiol. 133, 16–20.
Srinath, E.G., Sastry, C.A., Pillai, S.C., 1959. Rapid removal of phosphorus from sewage by activated sludge. Cell. Mol. Life Sci. 15, 339–340.
Thompson, P.A., Guo, M.x., Harrison, P.J., 1992. Effects of variation in temperature. I. On the biochemical composition of eight species of marine phytoplankton. J. Phycol. 28, 481–488.
Tien, C.J., Sigee, D.C., White, K.N., 2005. Copper adsorption kinetics of cultured algal cells and freshwater phytoplankton with emphasis on cell surface characteristics. J. Appl. Phycol. 17, 379–389.
Wang, Y., Gan, N., Zhou, Y., Li, T., Cao, Y., Chen, Y., 2017. Novel single-stranded DNA binding protein-assisted fluorescence aptamer switch based on FRET for homogeneous detection of antibiotics. Biosens. Bioelectron. 87, 508–513.
Wanner, O., Gujer, W., 1986. A multispecies biofilm model. Biotechnol. Bioeng. 28, 314–328.
Yao, B., Xi, B., Hu, C., Huo, S., Su, J., Liu, H., 2011. A model and experimental study of phosphate uptake kinetics in algae: considering surface adsorption and P-stress. J. Environ. Sci. 23, 189–198.
Yeoman, S., Stephenson, T., Lester, J.N., Perry, R., 1988. The removal of phosphorus during wastewater treatment: a review. Environ. Pollut. 49, 183–233.
Zhang, H.L., Fang, W., Wang, Y.P., Sheng, G.P., Zeng, R.J., Li, W.W., Yu, H.Q., 2013. Phosphorus removal in an enhanced biological phosphorus removal process: roles of extracellular polymeric substances. Environ. Sci. Technol. 47, 11482–11489.
Zhou, Y., Nguyen, B.T., Lai, Y.S., Zhou, C., Xia, S., Rittmann, B.E., 2016a. Using flow cytometry to evaluate thermal extraction of EPS from *Synechocystis* sp. PCC

6803. Algal Res. 20, 276–281.
Zhou, Y., Nguyen, B.T., Zhou, C., Straka, L., Lai, Y.S., Xia, S., Rittmann, B.E., 2017a. The distribution of phosphorus and its transformations during batch growth of *Synechocystis*. Water Res. 122, 355–362.
Zhou, Y., Xia, S., Zhang, J., Nguyen, B.T., Zhang, Z., 2017b. Insight into the influences of pH value on Pb (II) removal by the biopolymer extracted from activated sludge. Chem. Eng. J. 308, 1098–1104.
Zhou, Y., Xia, S., Zhang, J., Zhang, Z., Hermanowicz, S.W., 2016b. Adsorption characterizations of biosorbent extracted from waste activated sludge for Pb (II) and Zn (II). Desalin. Water Treat. 57, 9343–9353.
Zhou, Y., Xia, S., Zhang, Z., Zhang, J., Hermanowicz, S.W., 2016c. Associated adsorption characteristics of Pb (II) and Zn (II) by a novel biosorbent extracted from waste-activated sludge. J. Environ. Eng. 142, 04016032.
Zhou, Y., Zhang, Z., Zhang, J., Xia, S., 2016d. Understanding key constituents and feature of the biopolymer in activated sludge responsible for binding heavy metals. Chem. Eng. J. 304, 527–532.